7.2-7.3 (s, 10 H); mass spectrum (mixture), m/z (rel intensity) 242 (8), 205-209 (100), 121 (100) (see Table IV).

2.7. Reaction of EtMgBr with α-Phenylbenzoin. A THF solution of 0.11 mmol of EtMgBr (0.42 M, 0.25 mL) was mixed with a THF solution of 0.05 mmol of α-phenylbenzoin (0.5 equiv) in a reaction vessel. The reacting solution became bright orange soon after the reactants were mixed. The EPR spectrum of the solution was the same as that of GCR observed in the reaction of PhMgBr with benzil in the ratios of B/G < 1.0.

2.8. Reaction of PhMgBr with α-Methylbenzoin. A THF solution of 0.24 mmol of PhMgBr (0.96 M, 0.25 mL) was mixed with a THF solution of 0.12 mmol of α-methylbenzoin (0.5 equiv) in a reaction vessel. The reacting solution became bright orange soon after the reactants were mixed. The EPR spectrum of the solution was the same as that of GCR observed in the reaction of MeMgBr with benzil mixed in the ratios of $0.3 \leq B/G \leq 0.5$.

2.9. Reaction of PhLi with Benzil. A ethyl ether solution of 0.17 mmol of PhLi (0.66 M, 0.25 mL) was mixed with 6 mL of a THF solution of benzil in a reaction vessel. In the reactions of excess benzil (B/PhLi > 1.0), the reacting solution became dark brown as soon as the reactants were mixed together and showed well-resolved EPR spectra of PCR with a g value of 2.0047. In the reactions of excess PhLi (B/PhLi < 1.0), the solutions became green soon after the reactants were mixed and showed very complex but well-resolved EPR spectra with a g value of 2.0031.

2.10. EPR Observations at 77 K. A known amount of EtMgBr or PhLi was mixed with a 2-methyltetrahydrofuran (MTHF) solution of benzil in a reaction vessel at room temperature. Then, the EPR quartz cell containing MTHF solution of PCR or GCR was placed in the tip of a quartz Dewar filled with liquid nitrogen, and the tip of the Dewar was inserted into a resonance cavity of EPR. The resulting EPR spectra of the PCRs and GCR at 77 K are shown in Figures 4 and 6, respectively. When we mixed the solvent with ethyl ether, the weak, fine structure of the PCR which appeared in the reaction of EtMgBr with benzil was enhanced; the phenomena might be related to the well-known fact that neutral Grignard reagents prefer to aggregate in ethyl ether.[7d]

2.11. Change of B/G in Situ. At solution B, PCR prepared in the mixing ratio of B/G = 2.0 (0.25 mL of a 0.42 M THF solution of EtMgBr was reacted with 2 equiv of benzil dissolved in 6 mL of THF) was left standing for 2 h before the subsequent experiments. When a calculated amount of EtMgBr solution (0.42 M, 0.17 mL) was added to the prepared sample to make the solution correspond to B/G = 1.2, the amount of the PCR decreased to 85% of the initial amount. When a calculated amount of EtMgBr solution (0.42 M, 0.38 mL) was added to another prpared sample as described above to give the value of B/G = 0.8, the solution became colorless or pale yellow, and the PCR vanished completely. This was confirmed not only by EPR but also by electronic spectra. Further, when into another prepared sample was added a calculated amount of EtMgBr solution (0.42 M, 0.58 mL) to give the value of B/G = 0.6, the PCR vanished immediately, and the solution became bright orange, indicating appearance of GCR.

3. Kinetic Observations by Stopped-Flow Method. All of the instruments were dried in vacuo and flushed with high purity argon before use. Samples were prepared in well-dried and argon-flushed vessels sealed with rubber septa. Grignard reagents were diluted with dry THF to $^1/_2$ or $^1/_4$ of the initial concentration. Several THF solutions of benzil of different concentrations were employed, but the B/G ratio was kept constant at B/G = $^1/_{10}$. With syringes the reactants were transferred to reservoirs of the equipment which were kept dry with the flow of high purity nitrogen. In every case, the result was accumulated 4-60 times, and the resulted curve was analyzed by inspecting both computer curve fitting and Guggenheim plot. Detailed conditions of the experiments are given in Table III.

Acknowledgment. We are greatly obliged to Professor Noboru Hirota, Kyoto University, for his discussions on the radical ion pair and to Professor Jun-ichi Hayami, Kyoto University, for use of stopped-flow equipment as well as his discussions on the reaction kinetics.

Registry No. 1 (R = Ph), 103852-41-1; **1** (R = Me), 103852-43-3; **1** (R = Et), 103852-49-9; **2** (R = Ph), 103852-45-5; **2** (R = Me), 103852-47-7; **2** (R = Et), 103852-51-3; PhMgBr, 100-58-3; MeMgBr, 75-16-1; EtMgBr, 925-90-6; PhLi, 591-51-5; $Ph_2C(OH)C(OH)Ph_2$, 464-72-2; $PhC(O)C(O)Ph^{-}\cdot/K^{+}$, 95515-29-0; $PhC(O)C(O)Ph^{-}\cdot/Na^{+}$, 34508-03-7; $PhC(O)C(O)Ph^{-}\cdot/^1/_2Mg^{2+}$, 103852-36-4; PhC(O)C(O)-Ph·$^3/_2$Na, 103852-37-5; $Ph_2C(OH)C(O)Ph$·PhLi, 103852-38-6; PhC-(O)C(O)Ph·PhLi, 103852-39-7; benzil, 134-81-6; α-phenylbenzoin, 4237-46-1; α-methylbenzoin, 5623-26-7; (±)-2,3-diphenylbutane-2,3-diol, 22985-90-6; *meso*-2,3-diphenylbutane-2,3-diol, 4217-65-6.

Effect of Cationic Surfactants on the Conformational Transition of Poly(methacrylic acid)

Deh-ying Chu and J. K. Thomas*

Contribution from the Department of Chemistry, University of Notre Dame, Notre Dame, Indiana 46556. *Received January 13, 1986*

Abstract: The interaction between poly(methacrylic acid) and alkyltrimethylammonium bromide, C_nTAB, cationic surfactants has been investigated in aqueous solutions of pH 8, by use of the photophysics of pyrene and its derivatives. Photophysical studies of these fluorescent probes, both steady-state and pulsed laser studies, show that a conformational transition of PMA is induced by C_nTAB. The surfactant induces a coiling up of PMA chains at pH 8, which takes place via a cooperative process. This effect takes places when the concentration of C_nTAB is above a critical aggregate concentration, CAC. The CAC is 1 or 2 orders of magnitude less than the cmc of the corresponding micelle. There is a significant effect of surfactant chain length and PMA concentration on the CAC, which provides information on the nature of the CAC and the mechanism of the PMA transition. A model is suggested for the aggregation of PMA-$C_{10}TAB$ based on experimental data. Studies show that the aggregate consists of about 100 $C_{10}TAB$ molecules and 1 coiled polymer chain.

Considerable interest has developed in polymer-surfactant systems both as models for membrane mimetic chemistry[1] and for the practical uses, e.g., in processes of enhanced oil recovery.[2] Early studies have mainly focused on the interaction between nonionic polymers and surfactants, e.g., poly(ethylene glycol), PEG,[3a] poly(ethylene oxide), PEO,[3b] or poly(*N*-vinylpyrrolidone), PNVP,[3c] and the anionic surfactant, sodium dodecyl sulfate, SDS. A great variety of experimental data exists, but the nature of the

(1) Fendler, J. H. *Membrane Mimetic Chemistry*; Wiley: New York, 1983.

(2) Taber, J. J. *Pure Appl. Chem.* **1980**, *52*, 1323.

(3) (a) Tokiwa, F.; Tsujii, K. *Bull. Chem. Soc. Jpn.* **1973**, *46*, 2684. (b) Shirahawa, K. *Colloid Polym. Sci.* **1974**, *252*, 978. Cabane, B. *J. Phys. Chem.* **1977**, *81*, 1639. Turro, N. J.; Baretz, B. H.; Kuo, P. L. *Macromolecules* **1984**, *17*, 1321. Zana, R.; Lianos, P.; Lang, J. *J. Phys. Chem.* **1985**, *89*, 41, and references therein. (c) Kresheck, G. C.; Hargraves, W. A. *J. Colloid Interf. Sci.* **1981**, *83*, 1.

0002-7863/86/1508-6270$01.50/0

surfactant–polymer association in these systems is relatively weak.

Reports concerning the interaction of polyelectrolytes with the surfactants of opposite charge are relatively few,[4] especially the interaction of the weak polyelectrolytes with cationic surfactants,[5] presumably because of the immanence of rapid and irreversible precipitation.

Poly(methacrylic acid), a weak polyelectrolyte, exhibits a marked pH-induced conformational transition,[6] which is absent in poly(acrylic acid), PAA.[5] At low pH (<3), the free polymerized acid is formed, and the polymer collapse into a tight hydrophobic coil. However, above pH 4, the polymer coil tends to open. At higher pH (~8), the carboxylic groups are almost completely ionized, and the PMA chain is stretched out due to the repulsion of these anionic groups. At low pH hydrophobic molecules are hosted by the polymer coil, a condition which disappears at higher pH.[7] For any practical use of the polymer as a host material, strongly acidic polymers are to be avoided, and a hydrophobic environment for guest molecules is required close to neutral pH. From a scientific viewpoint, the interaction between cationic surfactants with PMA will allow us to study the effect of conformation of polyelectrolyte on the aggregation process and also to study the effect of cationic surfactants on the conformational transition of PMA.

In order to extend previous work,[8] the effects of cationic surfactants on the conformational transition of PMA have been investigated, by the use of fluorescent probes such as pyrene and its positively and negatively charged derivatives. A new conformational transition has been observed; i.e., the stretched PMA chain at pH ~ 8 collapses on the addition of cationic surfactants. Of immediate interest is the nature of the new aggregate formed and the mechanism of the cooperative process that forms it.

Experimental Section

Polymer Materials. Poly(methacrylic acid), PMA, used in this work was purchased from Polyscience Inc. Stable concentrated polymer solutions were prepared as in a previous study.[8b] The molecular weight of PMA was measured by viscosity studies to be 1.1×10^4. The concentration of the polymer solutions used was of the order 0.01–2 g/L. The exact numbers are given at the appropriate places.

Surfactants. Alkyltrimethylammonium bromides C_nTAB, such as decyltrimethylammonium bromide, $C_{10}TAB$ (Eastman), dodecyltrimethylammonium bromide, $C_{12}TAB$ (Eastman), and cetyltrimethylammonium bromide, $C_{16}TAB$ (Sigma) were recrystallized from ethanol. Hexyltrimethylammonium bromide (C_6TAB) and octyltrimethylammonium bromide (C_8TAB) were synthesized by refluxing either 1-bromohexane or 1-bromooctane (Aldrich) with an excess of 25% (w/v) trimethylamine–methanol solution (Kodak) at 20 °C for 24 h and then freeze dried, washed several times with diethyl ether, and finally recrystallized twice from benzene. Cetyltrimethylammonium chloride, $C_{16}TAC$ (Kodak), and dodecyltrimethylammonium chloride, $C_{12}TAC$ (Kodak), were used as received.

Fluorescent Probes and Other Reagents. (1-Pyrenylbutyl)trimethylammonium bromide (C_4PN^+), (1-pyrenylundecyl)trimethylammonium iodide ($C_{11}PN^+$), 1-pyrenedecanoic acid (PyC_9COOH), and 1-pyrenesulfonic acid sodium salt ($PySO_3Na$) were used as received from Molecular Probes. Pyrene and 1-pyrenebutyric acid, PyC_3COOH (Kodak), were purified by triple and double recrystallization from ethanol, respectively. Tris(2,2′-bipyridine)ruthenium(II) chloride, $Ru(bpy)_3^{2+}$ (G. Fredrick Smith) was purified as described previously.[8b] Sodium iodide (Fisher), thallium(I) nitrate (Ventron Alfa), and tetrabutylammonium iodide, TBI (Eastman), were used as received. 1-Dodecylpyridium chloride, DPC (Matheson, Coleman & Bell), was used as a quencher and was purified by double recrystallization from ethanol.

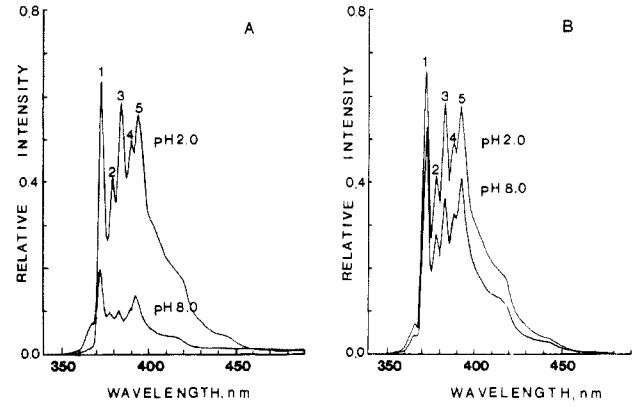

Figure 1. (A) Fluorescence spectra of pyrene in aqueous solutions of PMA at pH 2 and 8. [pyrene] = 2×10^{-6} M, [PMA] = 1 g/L. λ excitation = 340 nm. (B) Fluorescence spectra of pyrene in aqueous solutions of PMA at pH 2 and 8 containing 8×10^{-3} M $C_{10}TAB$. [pyrene] = 2×10^{-6} M, [PMA] = 1 g/L.

Sample Preparation. A typical procedure for preparing 2×10^{-6} M pyrene in an aqueous solution of aggregate of PMA–C_nTAB is as follows: 10 μL of a concentrated pyrene solution (2×10^{-3} M in EtOH) was added to a 10-mL volmetric flask and then was dried under a mild flow of air. After the solvent was evaporated, a calculated volume of stock concentrated PMA solution was added, diluted to 10 mL with deionized water, and stirred for 2 h. The pH of the solution was carefully adjusted to pH 8 by using concentrated NaOH and HCl solutions. A small quantity of concentrated C_nTAB solution was gradually added to the mixture from a syringe to give the required mixture composition, while keeping the mixture well stirred. Excessive addition of C_nTAB or a reverse order of preparation causes precipitation of a polymer–surfactant complex.

Measurements. Fluorescence decay rate constants were determined by a PRA LN-1000 nitrogen laser system with fast spectroscopic detection.[9] The fluorescence decay of pyrene and pyrene derivatives was monitored at 400 nm (λ); the luminescence decay of $Ru(bpy)_3^{2+}$ was monitored at 610 nm (λ). The quenching rate constants of excited pyrene were measured directly by the increased rate of decay of the excited pyrene on the addition of quencher. The overall observed rate constant, k_{obsd}, is related to k_o and k_q by the relationship $k_{obsd} = k_o + k_q[Q]$, where [Q] is the concentration of quencher and k_o and k_{obsd} are the first-order decay rate constants in the absence and in the presence of quencher, respectively. The slope of k_{obsd} vs. [Q] gives k_q.

The double-exponential decays were obtained by fitting time-dependent fluorescence data by an expression of the form

$$I(t) = I(0)[\alpha e^{-k_1 t} + (1 - \alpha)e^{-k_2 t}]$$

where k_1 and k_2 are the rate constants for two different exponential decays of the excited species and α indicates the fraction that decays with a faster rate constant k_1. $I(t)$ and $I(0)$ are the fluorescence intensities at time t and $t = 0$, respectively.

Fluorescence Polarization of 2-Methylanthracene. In this technique, the intensity of the fluorescence emission of 2-methylanthracene is measured at crossed (I_{vh}, I_{hv}) and parallel (I_{vv}, I_{hh}) positions of polarizing filters. The degree of polarization is given by[14c]

$$P = \frac{I_{vv} - I_{vh}(I_{hv}/I_{hh})}{I_{vv} + I_{vh}(I_{hv}/I_{hh})} 100\%$$

The subscripts denote the orientation of the electric vector of the light which passes the excitation (first letter) and emission (second letter) slit; v represents a vertical, h a horizontal orientation.

Steady-state fluorescence studies were carried out with a Perkin-Elmer MPF-44B fluorescence spectrophotometer. The relative fluorescence

(4) (a) Dubin, P. L.; Davis, D. D., et al. *J. Colloid Interf. Sci.* **1983**, *95*, 453; **1985**, *105*, 509; *Macromolecules* **1984**, *17*, 1294. Leung, P. S.; Goddard, E. D. et al. *Colloid Surf.* **1985**, *13*, 47, 63. (b) Abuin, E. B.; Scaiano, J. C. *J. Am. Chem. Soc.* **1984**, *106*, 6274. (c) Hayakawa, K; Kwak, J. C. T. *J. Phys. Chem.* **1982**, *86*, 3866.

(5) Hayakawa, K.; Santerre, J. P.; Kwak, J. C. T. *Macromolecules* **1983**, *16*, 1642.

(6) Katchalsky, A.; Eisenberg, H. *J. Polym. Sci.* **1951**, *6*, 145. Silberberg, A.; Eliassaf, J.; Katchalsky, A. *J. Polym. Sci.* **1957**, *23*, 259. Okamoto, H.; Wada, Y. *J. Polym. Sci., Part A-2*, **1974**, *12*, 2413 and references therein.

(7) (a) Barone, G.; Crescenzi, V.; Quadrifoglio, F. *J. Phys. Chem.* **1967**, *71*, 2341. (b) Chen, T.; Thomas, J. K. *J. Polym. Sci., Part A-1* **1979**, *17*, 1103.

(8) (a) Chu, D. Y.; Thomas, J. K. *Macromolecules* **1984**, *17*, 2142. (b) Chu, D. Y.; Thomas, J. K. *J. Phys. Chem.* **1985**, *89*, 4065.

(9) Hashimoto, S.; Thomas, J. K. *J. Am. Chem. Soc.* **1985**, *107*, 4655.

(10) Kalyanasundaram, K.; Thomas, J. K. *J. Am. Chem. Soc.* **1977**, *99*, 2039 and references therein.

(11) Thomas, J. K. *The Chemistry of Excitation at Interfaces*; ACS Monograph 181; American Chemical Society: Washington, DC, 1984.

(12) Atik, S. S.; Singer, L. A. *Chem. Phys. Lett.* **1978**, *59*, 519.

(13) Tabtar, H. V. *J. Colloid Interf. Sci.* **1959**, *14*, 115.

(14) (a) Shinitzky, M.; Dianoux, A. C.; Gitler, C.; Weber, G. *Biochemistry* **1971**, *10*, 2106. Cogan, U.; Shinitzky, M.; Weber, G.; Nishida, T. *Biochemistry* **1973**, *12*, 521. (b) Grätzel, M.; Thomas, J. K. *J. Am. Chem. Soc.* **1973**, *95*, 6885. (c) Azumi, T.; McGlynn, S. P. *J. Chem. Phys.* **1962**, *37*, 2413.

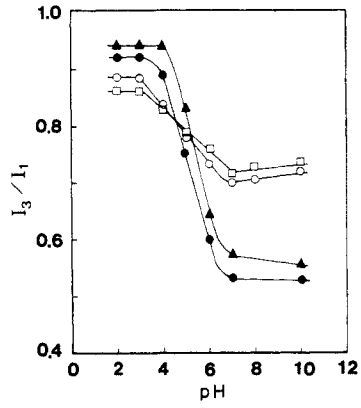

Figure 2. Effect of quaternary ammonium cationic surfactants on the intensity ratio, I_3/I_1, of pyrene fluorescence in aqueous solutions of PMA with pH: (▲) in the absence of quaternary ammonium salt, (●) in the presence of 1×10^{-2} M TBI, (○) in the presence of 1×10^{-2} M C_{10}TAB, (□) in the presence of 2×10^{-3} M C_{12}TAB. [PMA] = 1 g/L, [pyrene] = 2×10^{-6} M.

intensity of pyrene, I_r, is taken as the intensity of peak 1 ($\lambda \sim 373$ nm). The ratio I_3/I_1 is the ratio of the intensities of peak 3 ($\lambda \sim 384$ nm) to peak 1 ($\lambda \sim 373$ nm). The excitation wavelengths for pyrene and $C_{11}PN^+$ were 340 and 313 nm, respectively; there was less than 5% change in the absorbance at these wavelengths on addition of C_{10}TAB to PMA–pyrene solutions at pH 8. The absorption spectra were recorded on a Perkin-Elmer 552 spectrophotometer.

Results and Discussion

Influence of C_nTAB on the Conformational Transition of PMA Induced by pH. Previous studies have shown that poly(methacrylic acid) chains tend to open at pH > 4 and no longer exist as compact coils.[6] Earlier fluorescence studies using pyrene solubilized in PMA indicated that a sharp change in photophysical properties occurs as the polymer opens (pH > 4). When this happens, pyrene is ejected into the aqueous phase, where it exhibits a decreased fluorescence intensity and lifetime compared to hydrophobic environments.[7b] The data given in Figure 1 show fluorescence spectra of pyrene in aqueous solutions of PMA at pH 2 and 8, in the absence (A) and in the presence (B) of 8×10^{-3} M C_{10}TAB, respectively. The pyrene fluorescence spectrum consists of five peaks, labeled 1–5. The ratio of the relative intensities of peak 3 to peak 1 can be used to discuss the environmental effects on pyrene monomer fluorescence, the higher values of I_3/I_1 indicating the more hydrophobic environments for pyrene.[10] In the absence of C_{10}TAB, the fluorescence spectra of pyrene show dramatic changes over the range pH 2–8; I_r and I_3/I_1 are both lower at pH 8 than at pH 2. The fluorescence spectrum of pyrene in aqueous PMA at pH 8 is similar to that in water ($I_3/I_1 \simeq 0.53$). However, the fluorescence spectrum at pH 8 is quite different when C_{10}TAB is present (compare Figure 1B and Figure 1A). Both I_r and I_3/I_1 are much higher in the presence of 8×10^{-3} M C_{10}TAB compared to PMA solutions. These data indicate that pyrene is not ejected into the water phase in the presence of C_{10}TAB but still remains in a hydrophobic environment. The concentration of C_{10}TAB added in the foregoing experiments is much lower than the critical micelle concentration, cmc, of C_{10}TAB (6.5×10^{-2} M). As PMA does not host pyrene at pH 8, then it remains to suggest an interaction between C_{10}TAB and PMA which provides a hydrophobic region to host pyrene.

Figure 2 shows the effect of quaternary ammonium salts on the fluorescence ratio I_3/I_1 of pyrene in aqueous solutions of PMA as a function of pH. A sharp decrease is observed at pH ~ 4 for short-chain surfactants. In the presence of C_{10}TAB or C_{12}TAB, at concentrations that are far less than the cmc's of these surfactants, little decrease in the ratio I_3/I_1 is observed at pH > 4. These data contrast with those observed in PMA alone and in the PMA solutions containing the short-chain quaternary ammonium salts such as TBI (1×10^{-1} M). These data point out that the effects of quaternary ammonium salts on the PMA pH-induced transition are related to surfactant chain length.

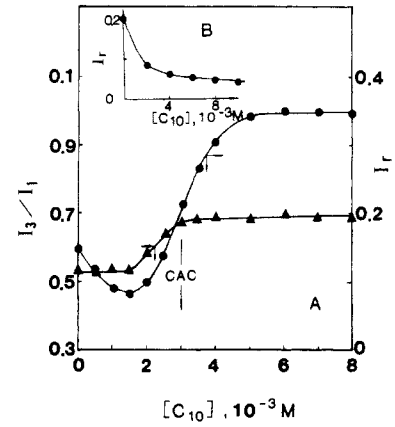

Figure 3. (A) Relative intensity of fluorescence, I_r (●), and intensity ratio, I_3/I_1 (▲), of pyrene as functions of concentrations of C_{10}TAB, $[C_{10}]$, in aqueous solutions of PMA at pH 8. [PMA] = 1 g/L, [pyrene] = 2×10^{-6} M. (B) Relationship between I_r of pyrene fluorescence and $[C_{10}]$ in water.

Table I. Effect of Concentration of C_{10}TAB on Decay Rate Constants[a] of Pyrene in Aqueous Solutions of PMA[b]

$[C_{10}TAB]$, 10^{-3} M	k_1, 10^6 s^{-1}	k_2, 10^6 s^{-1}	α
0		4.8	0[c]
1	20	4	0.6
2	20	4	0.7
3	8	2.6	0.4
4	8	2.6	0.3
5	8	2.6	0.22
6	8	2.6	0.17
7	8	2.6	0.13
8		2.8	0[c]

[a] Double-exponential decay. [b] In deaerated solutions at pH 8, [PMA] = 1 g/L, [pyrene] = 2×10^{-6} M. [c] $\alpha = 0$ means that the decay is single exponential in that case.

Critical Aggregate Concentration (CAC). Figure 3 shows the variation of I_r and I_3/I_1 for 2×10^{-6} M pyrene as a function of C_{10}TAB concentration in aqueous PMA solutions at pH 8. The curves show a sharp increase both in I_r and I_3/I_1 over a narrow range of C_{10}TAB concentrations. It is noted that the ratio I_3/I_1 in PMA–C_{10}TAB solutions reaches a steady value (~0.70) at a C_{10}TAB concentration, which is called a critical aggregate concentration, CAC. At the CAC, the hydrophobic aggregates of C_{10}TAB and PMA are formed which host hydrophobic molecules such as pyrene. The CAC corresponds to the midpoint of the transition in a plot of I_r vs. $[C_{10}]$. Table I shows the effect of C_{10}TAB concentration on the decay rate constants of pyrene fluorescence in systems used in Figure 3. The decay rate constants in Table I sharply decrease at a C_{10}TAB concentration of 3×10^{-3} M, which is in good agreement with the CAC determined via fluorescence I_3/I_1 measurement. As earlier studies of the PEO–SDS system,[3b] this again indicates that techniques that have been successfully used for cmc measurements in micellar systems[10] can also be used to investigate the aggregates of PMA and C_{10}TAB. Figure 3 and Table I show that the initial addition of C_{10}TAB (<CAC) causes a decrease in I_r, a decrease in the pyrene fluorescence intensity, and an increase in the decay rate constants, due to quenching by the free bromide ions. These data also show that pyrene is not associated with PMA or solubilized in PMA at pH 8 but is solubilized in the water phase. However, at C_{10}TAB concentrations above the CAC, pyrene is preferentially solubilized in hydrophobic regions formed by the aggregates of PMA–C_{10}TAB. Here, it is suggested that excited pyrene is protected from quenching by bromide in the aqueous phase; I_r and the lifetime therefore increase sharply.[4b]

There are a few reports on the interaction between strong anionic polyelectrolytes, such as sodium poly(styrene sulfonate), PSS, and the cationic surfactant dodecyltrimethylammonium bromide, C_{12}TAB, via a potentiometric technique[4c] and by luminescence studies.[4b] It is shown that the interaction between

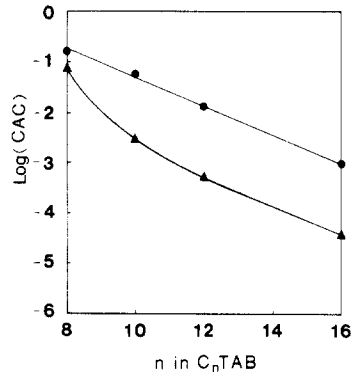

Figure 4. Plot of log (CAC) vs. n in C_nTAB (▲) and plot of log (cmc) vs. n in C_nTAB (●).

Table II. Effect of Chain Length of Cationic Surfactants on the CAC[a] and ΔG_A[b]

n in C_nTAB	CAC, M	ΔG_A, kcal mol^{-1}	cmc,[c] M	ΔG_M, kcal mol^{-1}
8	6×10^{-2}	−1.6	1.5×10^{-1}	−1.1
10	3×10^{-3}	−3.4	6.5×10^{-2}	−1.6
12	5×10^{-4}	−4.4	1.5×10^{-2}	−2.4
16	0.5×10^{-4}	−5.8	9.2×10^{-4}	−4.1

[a] CAC, the critical aggregate concentration of cationic surfactants C_nTAB in the aggregate of C_nTAB and PMA (pH 8, 1 g/L). [b] Free energy is calculated by $\Delta G_A = RT$ ln (CAC) and $\Delta G_M = Rt$ ln (cmc), $R = 1.987$ cal T^{-1} M^{-1}, $T = 293$ K. [c] Taken from ref 13.

polyelectrolytes and surfactants of opposite charge is highly cooperative and strong. The aggregation between PSS and $C_{12}TAB$ takes place well below the cmc of $C_{12}TAB$. However, there is no report on surfactant chain-length effect on the interaction between surfactants and polyelectrolytes. The present study indicates that the interaction between PMA and cationic surfactants is significantly dependent on chain length.

Chain-Length Dependence of CAC. Figure 4 shows a plot of log (CAC) vs. the number of carbon atoms of a cationic surfactant molecule, alkyltrimethylammonium bromide, (C_nTAB), and log (cmc) is also plotted as dashed line for sake of comparison. The figure shows that each CAC is markedly lower than the corresponding cmc of the surfactant. This is particularly true for $C_{10}TAB$, $C_{12}TAB$, and $C_{16}TAB$ (where the CACs are 1 to 2 orders of magnitude lower than the cmc!). Similar experiments in C_6TAB–PMA did not lead to an increase in I_r and I_3/I_1 up to surfactant concentrations of 0.5 M. The CAC for the C_8 surfactant is close to the cmc of the C_8TAB micelle, while TBI doesn't affect the conformational transition induced by pH. The above experiments tend to indicate that the interaction between PMA and cationic surfactants is chain length dependent. The shorter the chain length of C_nTAB, the weaker the interaction between C_nTAB and PMA, giving rise to a larger CAC. The measured CAC and a calculated ΔG_A, the free-energy change when the surfactant molecules are transferred from the aqueous phase to an aggregate of PMA–C_nTAB, are given in Table II. This latter parameter was calculated from the relationship $G_A = G_0 + RT$ ln (CAC) at the CAC; thus $\Delta G_A = RT$ ln (CAC). The absolute values of all ΔG_A are larger than the corresponding micellar values, ΔG_M, indicating a greater driving force for the formation of PMA–C_nTAB aggregates than that for micellization of C_nTAB.

Mechanism of the Conformational Transition of PMA Induced by Cationic Surfactants. The interaction between cationic surfactants and negatively charged polymers, e.g., PMA, decreases the negative charge densities of the polyelectrolyte. The cationic surfactant induces a phase transition in the polymer much akin to that produced by pH. This process is a cooperative one. The photophysical data show sharp changes over a narrow range of surfactant concentration, i.e., CAC data that are similar to cmc data. It is suggested that a cooperative process takes place consisting of a coiling of the polymer assisted by reduced charge density and the hydrophobic interactions of the surfactant chains

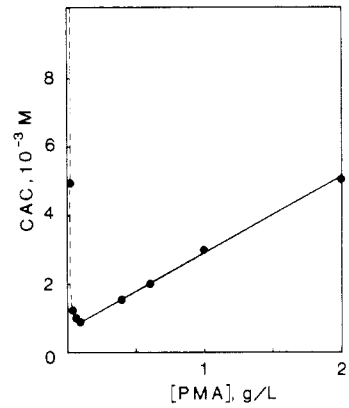

Figure 5. Dependence of the CAC of $C_{10}TAB$ in aqueous solutions of PMA on the concentration of [PMA], g/L.

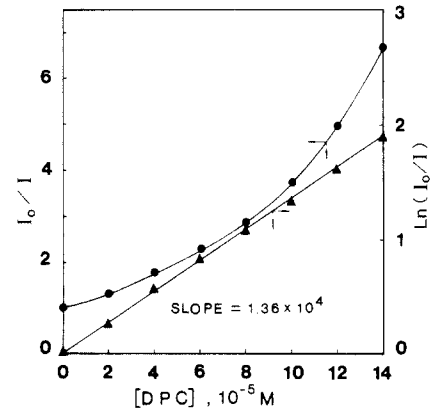

Figure 6. Quenching of pyrene fluorescence by DPC in PMA-deaerated aqueous solutions containing 8×10^{-3} M $C_{10}TAB$ at pH 8, calculated from steady-state data. [PMA] = 1 g/L, [pyrene] = 2×10^{-6} M. I_0 and I are relative intensities of pyrene fluorescence in the absence of and in the presence of DPC, respectively. Note: Plot of I_0/I (●) vs. [DPC] is not linear, but plot of ln (I_0/I) (▲) vs. [DPC] is linear and slope = 1.36×10^4.

bound to PMA. The surfactant $C_{10}TAB$ was chosen for further detailed studies.

Figure 5 shows the dependence of the CAC of $C_{10}TAB$ in aqueous PMA solutions on the concentration of PMA (g/L). The data show that a plot of CAC vs. [PMA] follows the stoichiometric relationship CAC (10^{-3} M) = 0.7 + 2.2 [PMA] (0.1 g/L < [PMA] ≤ 2 g/L). These data confirm that the polymer acts not as an inert additive in a micellar system but as an important component in aggregate formation. The higher concentrations of PMA require the higher $C_{10}TAB$ concentrations in order to induce the conformational transition of the PMA. Solutions of PMA at less than 0.1 g/L do not fit the above relationship, and the CAC increases and approaches the cmc (see the dashed line in Figure 5). This is due to the poor solubilization characteristics of such a low [PMA]. At the higher concentration of PMA, over 2 g/L, the solution at pH 8 becomes too viscous to handle the system for rapid mixing, etc., and precipitation readily occurs. It is not possible to measure a meaningful CAC in this solution.

It is also possible that the interactions between PMA and cationic surfactants merely increase the hydrophobic association between monomeric surfactants, which are assisted when the surfactants are together in close proximity in the polymer chain. This leads to random local small clusters of surfactants along the PMA chain, similar to other noncharged systems of PEO–SDS[3b] and strong polyelectrolyte PSS–$C_{12}TAB$.[4b] However, this possibility is ruled out in the PMA–$C_{10}TAB$ aggregate on the basis of the following experimental facts.

Mean Aggregation Number. The steady-state studies of the quenching of pyrene fluorescence by 1-dodecylpyridum chloride, DPC, in PMA aqueous solution of pH 8 containing 8×10^{-3} M $C_{10}TAB$ show that the data do not fit simple Stern–Volmer ki-

Table III. Rate Parameters Analyzed by Poisson Distribution for the Quenching of Pyrene Fluorescence by DPC in Aqueous Solutions of PMA Containing $C_{10}TAB$[a]

[DPC], 10^{-4} M	k_0, 10^6 s^{-1}	k_q, 10^7 s^{-1}	$\bar{n}$[b] calcd	[DPD][c]/[aggregate]	$\bar{N}$[d] calcd
0.2	2.7	2.0	0.27	0.27	108
0.4	2.7	2.0	0.54	0.55	108
0.6	2.7	2.0	0.78	0.83	104
0.8	2.7	2.0	0.93	1.08	93
1.0	2.7	2.2	1.15	1.35	92
1.2	2.6	2.2	1.35	1.60	90
1.4	2.6	2.2	1.75	1.90	100

[a] In deaerated solutions, [PMA] = 1 g/L, $[C_{10}TAB] = 8 \times 10^{-3}$ M, pH 8. [b] Quenching is measured by the pulsed studies. $\bar{n}$ is calculated from the Poisson quenching fit equation (2). $\bar{n}$ means molecules of quencher solubilized in each aggregate. [c] [aggregate] is measured by steady-state experiments, by eq 1. [d] $\bar{N}$ = aggregation number of C_{10}-TAB in the aggregate of PMA and $C_{10}TAB$, calculated by eq 3. Note: $\bar{N}$ from the steady-state experiment is 105 ± 10.

Table IV. Comparison of Decay Rate Constants of Pyrene Fluorescence between in Micelles (k_M) and in Aggregates of $C_{10}TAB$ with PMA (k_A)

n in C_nTAB	k_M, 10^6 s^{-1}[a]	k_A, 10^6 s^{-1}[b]
8	6.2	3.7
10	5.9	2.8
12	6.3	2.8
16	6.7	$k_1 = 18$, $k_2 = 3$, $\alpha = 0.55$[c]

[a] In deaerated cationic micellar solutions. $[C_8TAB] = 2 \times 10^{-1}$ M, $[C_{10}TAB] = 1.2 \times 10^{-1}$ M, $[C_{12}TAB] = 1.4 \times 10^{-2}$ M, $[C_{16}TAB] = 4.5 \times 10^{-3}$ M. [b] Surfactants in deaerated aqueous solutions of PMA at pH 8, [PMA] = 1 g/L. $[C_8TAB] = 1 \times 10^{-1}$ M, $[C_{10}TAB] = 8 \times 10^{-3}$ M, $[C_{12}TAB] = 2 \times 10^{-3}$ M, $[C_{16}TAB] = 8 \times 10^{-5}$ M. [c] Double-exponential decay.

netics; i.e., a plot of I_0/I vs. [DPC] is not linear. The data do fit a modified plot where ln (I_0/I) vs. [DPC] is linear (see Figure 6). This behavior is indicative of a Poisson distribution of quencher molecules amongst the aggregates. Analysis of these data according to this approach is achieved by using eq 1.[11] Since

$$\ln (I_0/I) = [\text{DPC}]/[\text{aggregate}] \quad (1)$$

the slope of ln (I_0/I) vs. [DPC] is 1/[aggregate] and the concentration of $C_{10}TAB$ is known, then the aggregation number of $C_{10}TAB$ as an aggregate can be calculated by $\bar{N} = [C_{10}TAB]/[\text{aggregate}] = 8 \times 10^{-3} \times 1.36 \times 10^4 = 109$. Similar experiments were done at different PMA concentrations, and $\bar{N} = 105 \pm 10$ was found as the average aggregation number.

Analysis of DPC quenching data via pulsed laser confirms the Poisson distribution of DPC amongst the aggregates. The data show an excellent fit of the Poisson kinetics to the time-dependent quenching of pyrene fluorescence in deaerated aqueous solutions of PMA at pH 8 that contained 8×10^{-3} $C_{10}TAB$ and quencher DPC. The time-dependent Poisson equation used is eq 2 where

$$I = I_0 \exp\{-k_0 t - \bar{n}[1 - \exp(-k_q t)]\} \quad (2)$$

$\bar{n}$ is the average number of DPC quencher molecules solubilized in each aggregate and k_0 and k_q are the first-order rate constants for the decay of pyrene in the absence and in the presence of quencher, respectively.[12] A more detailed analysis is shown in Table III. The values of $\bar{n}$ calculated by computer fitting of the Poisson kinetics are in good agreement with the numbers of [DPC]/[aggregate], where the [aggregate] is measured by steady-state studies (see Figure 6 and text above). The aggregation numbers of $C_{10}TAB$ in aggregates of PMA–$C_{10}TAB$ calculated by eq 3 are also shown in Table III. Those data correspond well

$$\frac{[C_{10}TAB]}{\bar{N}} = \frac{[\text{DPC}]}{\bar{n}_{\text{calcd}}} \quad (3)$$

to results from steady-state ($\bar{N} = 105 \pm 10$). Quenching studies of pyrene fluorescence by pyrene to give pyrene excimers also follow Poisson distribution and give similar values of $\bar{N}$ ($\bar{N} \sim 121$). The above experimental data confirm that the model for aggregation of PMA–$C_{10}TAB$ is not via local small and random clusters but is via larger discrete structures that are much larger than pure $C_{10}TAB$ micelles ($N \sim 36$).[13]

Nature of the Aggregates. The aggregates are hydrophobic, loose structures with some residual surface charge from the anionic polymer. A comparison of fluorescence decay rate constants of pyrene in micelles and in aggregates of PMA and C_nTAB is given in Table IV. The data show that the natural decay of pyrene fluorescence in aggregates is slower than in the C_nTAB micelle, i.e., $k_A < k_M$. This is due to the large amount of the quencher Br^- counterions in the micellar surface compared to some of the anionic PMA–$C_{10}TAB$ surface. The probe pyrene is located in the coiled aggregate away from the aqueous bromide ions. Meanwhile, k_A, the decay constant in aggregates, is identical with k_M in alkyltrimethylammonium chloride, C_nTAC (e.g., 2.9×10^6 s^{-1} in $C_{12}TAC$ and 3.2×10^6 s^{-1} in $C_{16}TAC$). It is noted that k_0 in PMA at pH 8 is 5.0×10^6 s^{-1} and similar to that in water. On the basis of the above data and the I_3/I_1 values presented in Figure 1B, 2, and 3, it is concluded that the interior of aggregate PMA–C_nTAB is hydrophobic and similar to that of a micelle. However, the Br^- counterions are in bulk aqueous phase.

The decay rate constants of several fluorescent probes are summarized in Table V and provide further evidence about the hydrophobic structure of the PMA–$C_{10}TAB$ aggregates. In the case of PMA (pH 8), k_0 is identical with k_0 in water, corresponding to previous studies which showed that the PMA chain is totally open at pH 8. There is one exception among the probes, i.e., $C_{11}PN^+$, which exhibits a double-exponential decay. (See next section for explanation.) On the other hand, all the k_0 in the PMA–$C_{10}TAB$ aggregates are closer or similar to those found in hexanol or in PMA at pH 3. The longer the carbon chain of the probe, the closer becomes the agreement of k_0 in hexanol and in aggregates. This is reasonable from the point of view of the hydrophobic effects involved. $Ru(bpy)_3^{2+}$ is too hydrophilic to locate in the interior of an aggregate, and its decay is similar to that in water. $(Ru(bpy)_3^{2+}$ in PMA at pH 5 is a special situation.[8b]) The quenching data show that the surface of the PMA–$C_{10}TAB$ aggregate has little charge, and the kinetic data are similar to those found in nonionic micelles.

The fluorescence of 2-methylanthracene, which can exhibit large polarization in rigid environment,[14] was also used to provide further information on the PMA–$C_{10}TAB$ aggregate. The degree of polarization of 2-methylanthracene as measured in various systems

Table V. Decay Rate Constants of Fluorescence of Several Fluorescent Probes

	k_0, 10^7 s^{-1}[a]				
	PMA[b]				
probe	pH 3	pH 8	pH 8 + $C_{10}TAB$[c]	hexanol	water
$PySO_3Na$	1.59	1.59	0.98	0.71	1.60
PyC_3H_7COOH	0.42	0.82	0.62	0.45	0.80
$PyC_9H_{19}COOH$	0.48	0.90	0.52	0.43	0.87
pyrene	0.24	0.48	0.28	0.26	0.48
$Ru(bpy)_3^{2+}$	$k_1 = 0.17$, $k_2 = 0.07$, $\alpha = 0.5$[d]	0.17	0.18	0.12	0.17
$C_4H_9PN^+$	0.41	0.75	0.53	0.44	0.70
$C_{11}H_{23}PN^+$	0.50	$k_1 = 10.0$, $k_2 = 0.7$, $\alpha = 0.4$[d]	0.50	0.53	0.78

[a] In deaerated solutions. [b] [PMA] = 1 g/L. [c] Aqueous solutions of PMA at pH 8 containing 8×10^{-3} M $C_{10}TAB$. [d] Double-exponential decay.

Table VI. Degree of Polarization (P) of 2-Methylanthracene[a] Fluorescence

system	P, %
PMA[b] at pH 2	17.1
PMA[b] at pH 3	14.7
$C_{10}TAB$ micelle[c]	7.5
PMA–$C_{10}TAB$[c]	4.4
cyclohexane	<0.5

[a] [2-Methylanthracene] = 2×10^{-6} M. [b] [PMA] = 1 g/L. [c] [$C_{10}TAB$] = 1×10^{-1} M. [d] Aqueous solutions of PMA (1 g/L) at pH 8, containing 8×10^{-3} M $C_{10}TAB$.

Table VII. Biomolecular Quenching Rate Constants of Pyrene Fluorescence

quencher Q	k_q,[a] 10^9 M^{-1} s^{-1} PMA (pH 8)–$C_{10}TAB$[c]	k_q,[a] 10^9 M^{-1} s^{-1} water
Tl^+[b]	3.3	6.2
O_2	5.3	9.8
CH_3NO_2	2.8	9.5
I^-[b]	1.2	1.3

[a] By pulsed studies, calculated from the expression $k = k_0 + k_q[Q]$. [b] $Tl^+ = TlNO_3$, $I^- = NaI$. [c] [$C_{10}TAB$] = 8×10^{-3} M, [pyrene] = 2×10^{-6} M, [PMA] = 1 g/L.

is summarized in Table VI. The data show that the degree of polarization of the fluorescence in the PMA–$C_{10}TAB$ aggregate is much smaller than that in PMA at pH 2–3 and even smaller than that observed in pure micellar systems. This indicates that 2-methylanthracene experiences a much less rigid environment in the PMA–$C_{10}TAB$ aggregate than in the PMA alone at low pH or in micellar media. The probe is relatively free to move in the aggregate structure. This is in good agreement with the bimolecular quenching studies presented in Table VII. The quenching of pyrene fluorescence is diffusion controlled, with quenchers such as $TlNO_3$, O_2, CH_3NO_2, and NaI. The quenching rate constants of pyrene with these quenchers in an aggregate are similar or slightly lower than those measured in the water phase. As the rates are diffusion controlled, then they reflect on the ease of movement of the reactants in the particular host used. The data suggest that the penetration of the above quenchers to pyrene hosted in the aggregate is only slightly inhibited by the host aggregate. By comparison the quenching rate constants by CH_3NO_2 and O_2 in micelles are nearly 1 order of magnitude smaller than those in water or alcohol and reflect on the more rigid environment of the micelle.

$C_{11}PN^+$ in the Aggregates. A long-chain derivative of pyrene, $C_{11}PN^+$,[15] was also used to study the effect of positive charge on the interaction of a fluorescent probe with PMA itself and with aggregates of PMA–$C_{10}TAB$.

The fluorescence spectra of 2×10^{-6} M $C_{11}PN^+$ is given in Figure 7. A large amount of pyrene excimer is formed at very low concentrations of $C_{11}PN^+$ in aqueous PMA solutions at pH 8 (spectrum b in Figure 7). Excimer formation indicates a clustering together of the hydrophobic $C_{11}PN^+$ molecules on the negatively charged PMA chain. However, in aggregate systems (Figure 7a), $C_{11}PN^+$ exhibits an enhanced monomer fluorescence spectrum with fine structures and a greatly reduced excimer spectrum.

The stacking or clustering together of $C_{11}PN^+$ in aqueous PMA solutions at pH 8 is also evident in the time-dependent emission of pyrene excimer at 480 nm. Formation of the excimer by migration of two pyrene molecules would require that the emission intensity increases over a period of time. However, for a stacked or clustered group of molecules, the excimer emission at 480 nm will be observed immediately following the laser excitation pulse. The experimental data show an immediate formation of the $C_{11}PN^+$ excimer in aqueous PMA solutions at pH 8, indicating a clustering of the $C_{11}PN^+$ molecules on the negatively charged polymer chain as discussed above.

(15) Atik, S. S.; Kwan, C. L.; Singer, L. A. *J. Am. Chem. Soc.* **1979**, *101*, 5696.

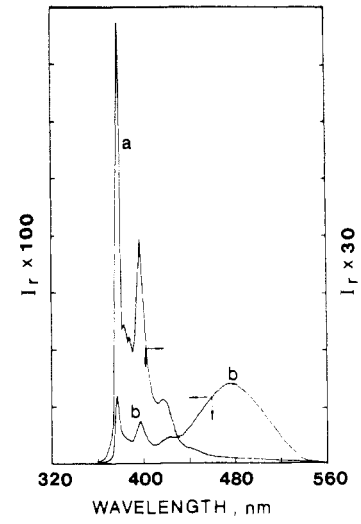

Figure 7. Fluorescence spectra of 2×10^{-6} M $C_{11}PN^+$ in aqueous solutions of PMA at pH 8 (a) containing 5×10^{-3} M $C_{10}TAB$ and (b) in the absence of $C_{10}TAB$.

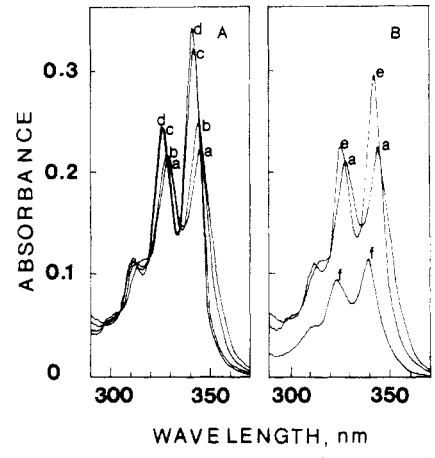

Figure 8. (A) Absorption spectra of 1×10^{-5} M $C_{11}PN^+$ in aqueous solutions of PMA at pH 8 on the addition of $C_{10}TAB$, 10^{-3} M: (a) 0, (b) 2.0, (c) 3.0, (d) 8.0. (B) Absorption spectra of 1×10^{-5} M $C_{11}PN^+$ in aqueous solutions of PMA at pH 8 (a), pH 2 (e), and in water (f).

On the addition of $C_{10}TAB$ to aqueous PMA solutions at pH 8, there is a dramatical enhancement of I_r (~377 nm) of $C_{11}PN^+$ fluorescence in the range 2×10^{-3}–4×10^{-3} M $C_{10}TAB$. The maximum yield of I_r with CAC is over 40 times larger than I_r in the absence of $C_{10}TAB$. The middle transition point (3.5×10^{-3} M) is close to the CAC (3×10^{-3} M) via measurements of I_3/I_1 and k_0, the pyrene fluorescence decay. However, in the absence of PMA, the initial addition of $C_{10}TAB$ causes a decrease in the I_r of $C_{11}PN^+$; thereafter the intensity increases as the $C_{10}TAB$ concentration goes above the cmc of the $C_{10}TAB$ micelle. The middle point of the transition (6×10^{-2} M) is in good agreement with the cmc of the $C_{10}TAB$ micelle (6.5×10^{-2} M).

The above data show that the I_r of $C_{11}PN^+$ vs. [surfactant] may also be used to estimate the CAC and cmc. The initial decrease in I_r with $C_{10}TAB$ was not observed in the presence of PMA, in contrast to the data in water. The chromophore $C_{11}PN^+$ in water is readily quenched by bromide ions on the addition of $C_{10}TAB$ below the cmc, but in aqueous PMA solution at pH 8, $C_{11}PN^+$ is electrostatically bound to PMA, while the negative charge of the polymer repels the bromide from the vicinity of the chromophore.

The absorption spectra of 1×10^{-5} M $C_{11}PN^+$ in aqueous PMA solutions at pH 8 on the addition of $C_{10}TAB$ are given in Figure 8. The absorption spectrum in PMA containing $C_{10}TAB$ below CAC (spectrum b) is similar to that in the absence of $C_{10}TAB$ (spectrum a) and shows a red shift compared to that in water (spectrum f). It is suggested that the red shift is due to the

electrostatic interaction between the ground states of $C_{11}PN^+$ and PMA at pH 8. It is also noted that the absorption spectrum is significantly and abruptly changed on the addition of $C_{10}TAB$ above the CAC. Spectra c and d show blue shifts compared to a and b but still show a red shift compared to that in water. It is also noted that there is a narrowing of all 0–0 transition bonds in the systems above the CAC, giving rise to an increase in the absorbance maxima. These trends are similar to the spectral charges observed in hydrophobic media such as compact PMA coils at pH 2 (spectrum e). None of the changes stated above for $C_{11}PN^+$ were observed in the case of pyrene.

Summary

This study shows that a conformational transition of PMA is induced by C_nTAB. The stretched PMA chain at pH 8 collapses on addition of the cationic surfactants, i.e., the cationic surfactants caused neutralized PMA chain refolding, thus providing a hydrophobic host place for fluorescent probes pyrene and/or its derivatives.

The hydrophobic aggregates are formed in cooperative processes once the surfactant concentration exceeds a certain concentration called the critical aggregation concentration, CAC, which is 1.4–1.7 orders of magnitude lower than the cmc of the C_nTAB micelle. The CAC is chain length dependent and also depends on the PMA concentration. On the basis of the measurements of the average aggregation number, decay rate constants, bimolecular quenching constants, and polarization studies, it is suggested that the aggregates of PMA–$C_{10}TAB$ are large structures consisting of about 100 $C_{10}TAB$ molecules and 1 coiled polymer chain. This is depicted as a hydrophobic but a loosely assembled structure with a surface of low-charge density. The interior of the aggregate has a hydrophobicity that is similar to that of micelle. However, the bromide ions are only in bulk aqueous phase and not close to the surface of the aggregate.

Studies using $C_{11}PN^+$ provide further information about the effect of positive charge on the interaction of the fluorescent probe with PMA chains (pH 8) and on the aggregate of PMA–$C_{10}TAB$. Both emission and absorption spectra show that the nature of the interaction and environment of $C_{11}PN^+$ are abruptly changed at concentrations of $C_{10}TAB$ above the CAC, i.e., from an electrostatic bonding with PMA chains in the water phase to solubilization in a hydrophobic aggregate.

This study also shows that the fluorescence probing technique is a very useful and powerful tool for investigations of conformational transition of polyelectrolytes as induced by cationic surfactants, pH, or other means.

Acknowledgment. We thank the National Science Foundation for support of this work via Grant CHE-01226-02.

Registry No. $C_{10}TAB$, 2082-84-0; $C_{12}TAB$, 1119-94-4; $C_{16}TAB$, 57-09-0; C_6TAB, 2650-53-5; C_8TAB, 2083-68-3; $C_{16}TAC$, 112-02-7; $C_{12}TAC$, 112-00-5; C_4PN^+, 81341-11-9; $C_{11}PN^+$, 103692-03-1; PyC_9COOH, 64701-47-9; $PySO_3Na$, 59323-54-5; $Ru(bpy)_3^{2+}2Cl^-$, 14323-06-9; $TlNO_3$, 10102-45-1; O_2, 7782-44-7; CH_3NO_2, 75-52-5; NaI, 7681-82-5; Py, 129-00-0; PyC_3COOH, 3443-45-6; poly(methacrylic acid), 25087-26-7.

A Photochemical Reaction Leading from Cyclohexenones to Cyclobutanones; Mechanistic and Exploratory Organic Photochemistry[1,2]

Howard E. Zimmerman* and Robert D. Solomon

Contribution from the Chemistry Department, University of Wisconsin, Madison, Wisconsin 53706. *Received January 16, 1986*

Abstract: In previous studies vinylcyclobutanones were encountered as minor products of the photochemistry of cyclohexenones. In the present investigation the structural features required for this reaction were explored. It was found that increased phenyl substitution at carbon five of the cyclohexenone enhanced cyclobutanone formation. Thus, in this study the photochemistry of 4,5,5-triphenylcyclohex-2-en-1-one and 4-methyl-5,5-diphenylcyclohex-2-en-1-one was investigated. In the triphenyl enone photochemistry, cyclobutanone formation reached 20% while in the methyl diphenyl enone case, cyclobutanone formation was the only process observed. The photolysis of 4,5,5-triphenylcyclohex-2-en-1-one led to 60% of 3,5,5-triphenylcyclohex-2-en-1-one, 16% of *exo*-4,4,6-triphenylbicyclo[3.1.0]hexan-2-one, 16% of 2-*trans*-styryl-3,3-diphenylcyclobutanone, and 4% of the *cis*-styryl cyclobutanone. The total quantum yield was 0.15. In the instance of the photochemistry of 4-methyl-5,5-diphenylcyclohex-2-en-1-one only 2-*trans*-propenyl-3,3-diphenylcyclobutanone was formed. The quantum yield in this case was 0.012. Acetophenone sensitization of the two enones led to the same products and efficiencies as observed for the direct irradiations. Triplet rates were measured. A test was devised to determine if a diradical mechanism or, alternatively, a 1,3-sigmatropic process was responsible for cyclobutanone formation. For this purpose the methyl diphenyl enone and its propenyl cyclobutanone product were resolved. Photolysis of the cyclohexenone afforded primarily racemic diphenyl propenyl cyclobutanone with residual 6% enantiomeric excess. Unreacted diphenyl cyclohexenone showed no racemization. Control runs showed vinyl cyclobutanone product was not racemizing under either photolysis or isolation conditions. This evidence suggested a mechanism involving fission of bond 4–5 to afford a diradical stabilized by the two C-5 phenyl groups. Attack of the diphenylmethyl radical center on C-2 then leads to cyclobutanone product. The slight residual chirality is attributed to a rate of diradical conformational equilibration not quite rapid enough to give complete racemization. A concerted 1,3-sigmatropic rearrangement mechanism, with benzhydryl migrating with equal probability on the two π-faces, is excluded by the exclusive formation of *trans*-propenyl product. The photochemistry of the triphenyl enone is also discussed from a mechanistic viewpoint. Finally, the ethylvinyloxy diradical is noted to be involved in a number of photochemical reactions.

The photochemistry of 4-aryl-substituted cyclohexenones has been a subject of considerable interest. The initial report[3a] revealed that irradiation of 4,4-diphenylcyclohexenone (**1**) led to *trans*-5,6-diphenylbicyclo[3.1.0]hexan-2-one (**2**) as the major product.

(1) This is Paper 149 of our photochemical series and Paper 207 of our general series.

(2) For Paper 148 see: Zimmerman, H. E.; Binkley, R. W. *Tetrahedron Lett.* **1985**, 5859–5862.

0002-7863/86/1508-6276$01.50/0